

Experimental study of coupled oscillations on a Slinky Wilberforce pendulum

Vinicius Dos Passos de Souza¹, Pedro Gonçalves Queiruga¹, Enesio Marinho Jr.^{*1,2}

¹Universidade Federal do ABC, Centro de Ciências Naturais e Humanas, 09210-580, Santo André, SP, Brasil.

²Universidade Estadual Paulista, Instituto de Física Teórica, 01140-070 SP, Brasil.

Received on January 27, 2022. Revised on March 13, 2022. April 19, 2022.

The Wilberforce pendulum is a mechanical oscillator often used to demonstrate the phenomenon of coupled oscillations. It is a spring-mass system whose pendulum bob contains lateral rods to vary its moment of inertia, being possible to verify the coupling of the rotational and longitudinal motions of the resonant system. In the present work, we present a experimental study of the coupled oscillations on the Wilberforce pendulum using easily accessible materials. With a *Slinky* spring toy, a wood rod containing masses at the extremities and getting images of the movements using a mirror and the TRACKER software on a smartphone, we could analyze quantitatively the properties associated with the coupled oscillations. The final result has indicated excellent agreement with the theoretical modeling, and therefore it can be used in teaching of wave physics.

Keywords: Wilberforce pendulum, coupled oscillations, energy conservation, wave physics.

1. Introduction

In physics, we usually come across such a variety of oscillating coupled systems. Actually, completely isolated oscillators is rarely verified in nature. For instance, a spring can be described as a ensemble of several constituent particles coupled with each other. The wave motion occurs due to neighbouring oscillating particles being coupled one to another, resulting in an energy transmission. Some examples of two coupled systems are: two simple pendulum with their bobs coupled using a spring, or two coupled *LC* circuits. These coupled systems are said to have two degrees of freedom [1]. The Wilberforce pendulum is a mass-spring oscillator proposed by Lionel R. Wilberforce in 1894 [2], consisting of a mass suspended by a helical spring that is free to oscillate in longitudinal and torsional modes [3]. In this sense, the Wilberforce pendulum is an example of a coupled mechanical oscillator that can be used to demonstrate the phenomenon of coupled oscillation in most introductory physics courses. A sketch of this mechanical oscillator is shown in Figure 1-A. Using this oscillator, it can be noticed that the pendulum has two motions: the translation and the rotation, whose intensities are coupled. It means that the vibrational energy in longitudinal direction is gradually transferred to torsional oscillation energy, and vice versa [4]. Thus, although being a relatively simple mass-spring oscillator, it is an excellent pedagogical apparatus to demonstrate some important wave physics principles [4, 5].

The equation of motion for the Wilberforce pendulum represents a linear combination of the longitudinal and torsional modes of vibration [3]:

$$\mathbf{R}(t) = z(t)\hat{z} + \theta(t)\hat{\theta}. \quad (1)$$

The results shown in Figure 1-B, taken from Ref. [3], describe the oscillations in both coordinates z and θ as a function of time. We can clearly observe the relationship between the phases of the coordinates as a result of the energy transfer. So that, the greater is amplitude in the coordinate θ , the smaller is the amplitude in the coordinate z , and vice versa.

Using digital techniques for the analysis of natural phenomena such as coupled oscillation is a modern method applied to design wave physics experiments [6].

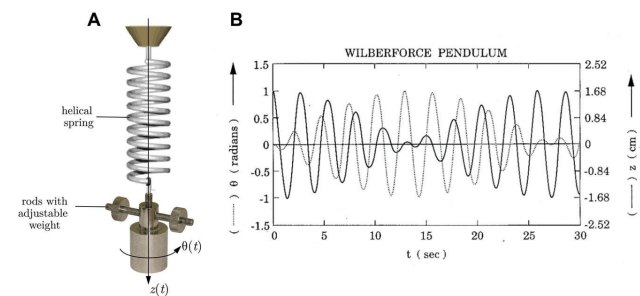


Figure 1: The Wilberforce pendulum and the coupled oscillation: (A) a sketch showing the coordinate system with the longitudinal $z(t)$ and torsional $\theta(t)$ directions. (B) Results for z and θ as a function of time for the Wilberforce pendulum, reproduced from Ref. [3], with the permission of the American Association of Physics Teachers.

* Correspondence email address: enesio.junior@ufabc.edu.br

In addition, the COVID-19 pandemic has suddenly and abruptly forced educational institutions to adopt some digital techniques to teach experiments and fundamental physics phenomena [6, 7].

In the present work, we describe an experimental implementation of the Wilberforce pendulum which was accurate enough to give quantitative insight into the fundamental oscillating properties. However, the experimental apparatus was intended to be simple enough to be reproduced by physics students only using easy accessible materials and a smartphone. The results have shown that we could quantitatively analyze the Wilberforce pendulum composed of a Slinky toy acting as a spring, a wooden rod with masses in its extremities. The coordinates for the translation and rotation motions were obtained using the TRACKER software installed in a smartphone.

2. Methods

2.1. Theoretical model

Let us consider a massless helical spring with spring constant k and torsional spring constant δ . As the pendulum bob, we hang a rod with masses at its extremities resulting in a moment of inertia I and total mass M . Assuming a linear coupling of oscillations being described by a potential in the form

$$U = \frac{1}{2}\epsilon z\theta, \quad (2)$$

where ϵ is the coupling constant, z and θ are the two coordinates, $z = \theta = 0$ is the equilibrium point. Thus, the Lagrangian of the pendulum can be written as [3]

$$\mathcal{L} = \frac{1}{2}(M\dot{z}^2 + I\dot{\theta}^2) - \frac{1}{2}(kz^2 + \delta\theta^2 + \epsilon z\theta), \quad (3)$$

where I is the moment of inertia of the system with respect to the vertical axis, δ is the torsion constant of the spring, and ϵ is the coupling constant between vertical and rotational oscillations [3, 5].

Applying the Euler-Lagrange equation,

$$\frac{d}{dt}\left(\frac{\partial\mathcal{L}}{\partial\dot{q}}\right) - \frac{\partial\mathcal{L}}{\partial q} = 0, \quad (4)$$

for $q = \{z, \theta\}$, we get from Eq. (3)

$$M\ddot{z} + kz + \frac{1}{2}\epsilon\theta = 0, \quad (5)$$

$$I\ddot{\theta} + \delta\theta + \frac{1}{2}\epsilon z = 0. \quad (6)$$

The Eqs. (5) and (6) describe the dynamics of the Wilberforce pendulum considering the coupled oscillation.

Assuming the solutions equal to those obtained for the simple harmonic oscillator,

$$\begin{aligned} z(t) &= A_1 \cos(\omega t + \varphi) \\ &= \text{Re}\{A_1 e^{i(\omega t + \varphi)}\}, \end{aligned} \quad (7)$$

$$\begin{aligned} \theta(t) &= A_2 \cos(\omega t + \varphi) \\ &= \text{Re}\{A_2 e^{i(\omega t + \varphi)}\}, \end{aligned} \quad (8)$$

in Eqs. (5) and (6), respectively, we get

$$\left(\frac{k}{M} - \omega^2\right)A_1 + \frac{\epsilon}{2M}A_2 = 0, \quad (9)$$

$$\frac{\epsilon}{2I}A_1 + \left(\frac{\delta}{I} - \omega^2\right)A_2 = 0, \quad (10)$$

and then defining

$$\omega_z \equiv \sqrt{\frac{k}{M}}, \quad (11)$$

$$\omega_\theta \equiv \sqrt{\frac{\delta}{I}}, \quad (12)$$

the expressions yield

$$(\omega_z^2 - \omega^2)A_1 + \frac{\epsilon}{2M}A_2 = 0, \quad (13)$$

$$\frac{\epsilon}{2I}A_1 + (\omega_\theta^2 - \omega^2)A_2 = 0. \quad (14)$$

To obtain non-trivial solutions, we must impose that the determinant

$$\begin{vmatrix} \omega_z^2 - \omega^2 & \frac{\epsilon}{2M} \\ \frac{\epsilon}{2I} & \omega_\theta^2 - \omega^2 \end{vmatrix} = 0, \quad (15)$$

which results in

$$\omega^4 - (\omega_z^2 - \omega_\theta^2)\omega^2 + \left(\omega_z^2\omega_\theta^2 - \frac{\epsilon^2}{4MI}\right) = 0. \quad (16)$$

Solving this equation for ω^2 , we obtain the two normal modes of vibration

$$\omega_+^2 = \frac{1}{2}\left[\omega_z^2 + \omega_\theta^2 + \sqrt{(\omega_z^2 - \omega_\theta^2)^2 + \frac{\epsilon^2}{MI}}\right], \quad (17)$$

$$\omega_-^2 = \frac{1}{2}\left[\omega_z^2 + \omega_\theta^2 - \sqrt{(\omega_z^2 - \omega_\theta^2)^2 + \frac{\epsilon^2}{MI}}\right]. \quad (18)$$

When the natural frequencies ω_z and ω_θ are equal, then for $\omega_z = \omega_\theta = \omega$ we get

$$\omega_+^2 = \omega^2 + \frac{\epsilon}{\sqrt{MI}}, \quad (19)$$

$$\omega_-^2 = \omega^2 - \frac{\epsilon}{\sqrt{MI}}. \quad (20)$$

In Eq. (13), considering the normal mode ω_1 replacing ω , and for $\omega_z = \omega$ when the oscillator is in resonance, therefore

$$\frac{\epsilon}{\sqrt{MI}}A_1 + \frac{\epsilon}{2M}A_2 = 0, \tag{21}$$

so that the ratio between the amplitudes reads

$$\frac{A_2}{A_1} = \sqrt{\frac{M}{I}}. \tag{22}$$

Eqs. (19) and (20) can be rewritten more compactly as [5]

$$\omega_{\pm}^2 = \omega^2 \pm \omega_b, \tag{23}$$

where ω_b is defined as

$$\omega_b \equiv \frac{\epsilon}{\sqrt{kI}} = \frac{\epsilon}{\sqrt{\delta M}}. \tag{24}$$

If we consider the situation in which the Wilberforce pendulum is released from equilibrium, with an initial longitudinal displacement A_1 , without initial phase and rotational amplitude. In this case, the solutions of the equations of motion will be [5]

$$z(t) = A_1 \cos\left(\frac{\omega_b t}{2}\right) \cos(\omega t), \tag{25}$$

$$\theta(t) = A_2 \sin\left(\frac{\omega_b t}{2}\right) \sin(\omega t), \tag{26}$$

in the weak coupling limit. Both of these equations take the form of a rapid oscillation at the natural frequency ω inside a slowly varying envelope [5, 8].

2.2. Prototypes

To study the coupled oscillations of the Wilberforce pendulum. The pendulum bob was attached at one end of the spring, and the other one was fixed on a stepladder used as a support.

The first prototype of the Wilberforce oscillator was made using a notebook metal spiral spring as a spring. As the pendulum bob, we used a soda can with attached screws that act as side rods and support the side hanging masses. This model is shown in Figure 2-A.

In the second prototype we used the slinky plastic spring, which was fixed by means of wires to a piece built with the acrylic ruler and pen, which will serve as a support for placing the lateral masses. This second prototype is shown in Figure 2-B.

Once with the two previous prototype we could get a reproducible coupled oscillation, we created a third prototype, obtained using the same slinky spring used in the second prototype. But in this final prototype, the pendulum bob was a bamboo pole with playdough at the ends of this pole. With this final prototype, depicted in Figure 2-C, we were able to verify the expected coupled oscillations.

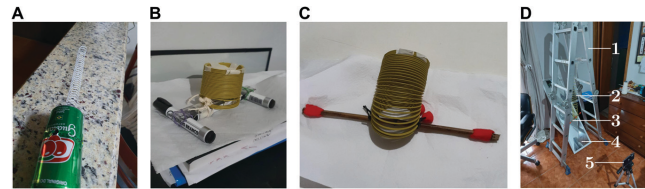


Figure 2: Prototypes and the experimental setup: first assembled Wilberforce pendulum prototypes using (A) a notebook spiral and (B) a slinky spring with acrylic ruler and markers as rods and weights. (C) Final prototype used for the quantitative analyses, comprising of a wood rod with playdough as masses at the extremities, resulting in a total pendulum bob of 14.0 ± 0.5 g. (D) Setup used for measurements of the coordinates, containing (1) a stepladder used as a support for the spring, (2) the slinky spring, (3) the pendulum bob with wood rod and weights, (4) a plane mirror to allow recording simultaneously the translation and the rotation, and (5) tripod with cellphone for video acquisition.

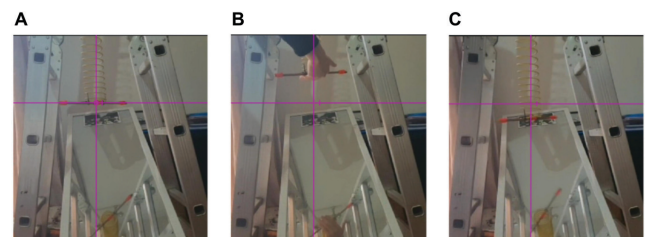


Figure 3: Experimental procedure carried out to record the coordinates for the Wilberforce pendulum. (a) First, the pendulum in equilibrium is recorded in order to set the referential point in z -axis. (b) Afterwards, we raise the pendulum bob a little, and (c) finally, we release the pendulum, starting the vertical oscillation. The magenta lines represent the axes used.

2.3. Experimental setup and measurement procedure

The experimental setup used to obtain the coupled oscillations is shown in Figure 2-D. We hung the slinky Wilberforce pendulum in a stepladder. To measure the masses of the pendulum bob, we have used a digital balance (Globalmix SF-400). We also used the TRACKER software [9] to record and analyze the coordinates z and θ during the coupled oscillations. In order to record simultaneously both the translation and rotational motions, we placed a plane mirror properly inclined ($\sim 45^\circ$) below the slinky Wilberforce pendulum, analogous to a previously reported study [10]. We use a smartphone on a tripod to acquire the images, thus ensuring stability in the recording.

First, the spring was raised vertically above its equilibrium point and then released to start the oscillations. Initial rotation is null. The steps showing the initial boundary conditions already being obtained by the TRACKER software are presented in Figure 3.

To obtain the fits for the experimental data, we used the SCIPY.OPTIMIZE library from python. Specifically,

we use the function `CURVE_FIT` which implements the nonlinear least squares method to fit a function and get the optimized parameters.

3. Results and Discussion

3.1. Spring characterization

The elastic constant of the spring can be estimated from the relationship between the added mass (in kilograms) and the corresponding deformation of the spring (in meters). In the equilibrium state of the spring-mass system, we have that the magnitude of the resulting force is the weight, which in this case will be equal to the elastic force:

$$F = Mg = kz, \quad (27)$$

where M is the mass supported by the spring, g is the acceleration of gravity (we used $g = 9.8 \text{ m/s}^2$), k the elastic constant of the spring and z the deformation of the spring. Rearranging the above expression, we get

$$M = \frac{k}{g}z. \quad (28)$$

Thus, from the adjustment of the experimental values of mass and deformation of the spring, it is possible to estimate the elastic constant of the spring by the angular coefficient obtained. Let α be the slope of the linear fit $M(z) = \alpha z$, the elastic constant can be calculated by,

$$\alpha = \frac{k}{g} \implies k = \alpha g. \quad (29)$$

We use nickels and dimes as masses. The results obtained from the deformation of the spring in relation to the added masses are shown as the experimental data in Figure 4. Based on these values, we obtained the linear fit shown in Figure 4 (solid line).

However, the best curve fit obtained for the mass data as a function of displacement was a parabolic fit in the form

$$M = Az^2 + Bz + C, \quad (30)$$

where $A = (0.018 \pm 0.001) \text{ kg m}^{-2}$, $B = (0.054 \pm 0.001) \text{ kg m}^{-1}$ and $C = (0.0019 \pm 0.0004) \text{ kg}$. This quadratic fit is shown in Figure 4 (dashed line). We expected to obtain a straight equation, but we ended up getting a quadratic fit as a result, thus showing that the spring has a load limit for which it has a linear behavior, cf. described by Hooke's law.

In this case, we estimated the linear behavior of the spring using the equation

$$M = Bz + C, \quad (31)$$

with the values of B and C obtained with the polynomial fit of second order. With that, we were able to calculate

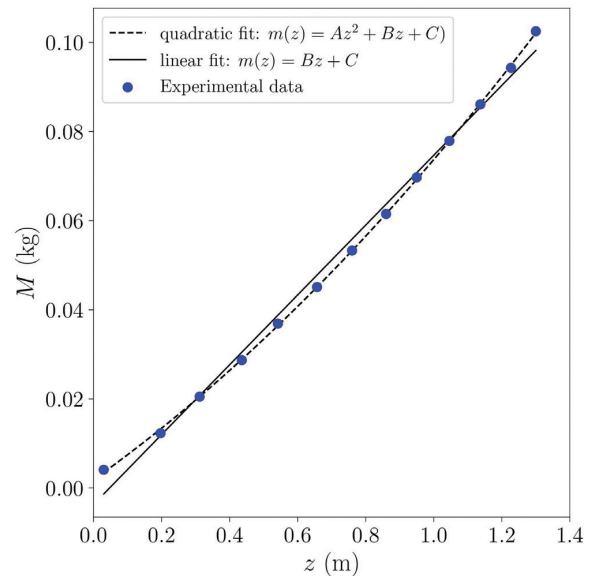


Figure 4: Characterization of the slinky spring. Mass data versus the longitudinal displacement were obtained experimentally (circles in blue). Linear and quadratic fits are represented by solid and dashed lines, respectively.

the spring constant using Eq. (29). Thus, we obtained as a result

$$k = (0.53 \pm 0.01) \text{ N m}^{-1}, \quad (32)$$

with uncertainty calculated from the error propagation in the elastic constant equation.

As shown in Figure 4, when we consider masses between $(8 \pm 0.5) \text{ g}$ and $\sim (80 \pm 0.5) \text{ g}$ we have a spring with a reasonable linear behavior. The first experimental data had a mass of $(4.1 \pm 0.5) \text{ g}$, which was quite similar to the one of spring $(\sim (3.0 \pm 0.5) \text{ g})$, making then the spring to have a non-linear behavior. That similarity in masses is not verified already for the second experimental data $((12.3 \pm 0.5) \text{ g})$. From the 10th mass $((77.9 \pm 0.5) \text{ g})$ and beyond, we can notice a non-linear behavior of the spring similar to a hard spring [11].

3.2. Moment of inertia of support

To estimate the moment of inertia of the support, we modeled the support with masses at the ends as shown in Figure 5. Thus, the moment of inertia will be given by

$$I_{\text{pendulum bob}} = I_{\text{rod}} + 2I_{\text{mass}}, \quad (33)$$

where I_{rod} is the moment of inertia of the horizontal rod and I_{mass} is the moment of inertia of the masses contained in the ends of the rod. Using moment of inertia of a solid bar and assuming that the weights are punctual, the moment of inertia reads

$$I_{\text{pendulum bob}} = \frac{1}{12}ML^2 + 2m\frac{L^2}{4}. \quad (34)$$

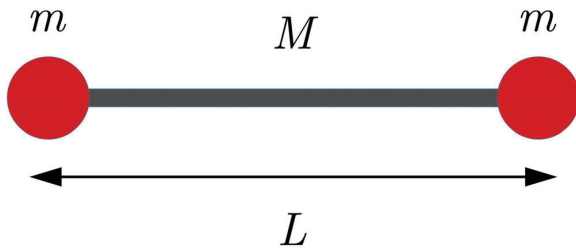


Figure 5: Schematic representation of the pendulum bob, with lateral masses m , bar mass M and bar width L .

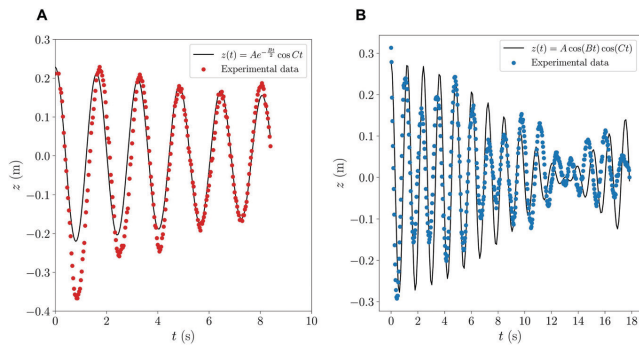


Figure 6: Vertical displacement curves z (in meters) as a function of time (in seconds) obtained using (A) the first pendulum prototype with a notebook spiral spring shown in Figure 2-A, and (B) results for the second prototype with the slinky spring with pens acting as masses depicted in Figure 2-B.

Substituting the measured values: $M = (4.0 \pm 0.5) \times 10^{-3}$ kg, $m = (5 \pm 0.5) \times 10^{-3}$ kg and $L = (30.0 \pm 0.05) \times 10^{-2}$ m (masses measured with a scale with a minimum measure of 1g and distance with a ruler with a smaller measure of 0.1 cm), and using the error propagation we were able to estimate the moment of inertia of

$$I_{\text{pendulum bob}} = (2.2 \pm 0.2) \times 10^{-4} \text{kg m}^2, \quad (35)$$

where the uncertainty was estimated from the error propagation.

3.3. Results of the oscillators

Initially, we analyzed the oscillations for the the first prototype, in which we used a notebook metal spiral spring (Figure 2-A). By recording and analyzing the dynamics of the translational motion, we verified a curve with behaviors different from the expected ones, recalling the solution of the equation of motion for a damped oscillator (Figure 6-A).

This is confirmed by the form of the curve fitting,

$$z(t) = De^{-\frac{\gamma t}{2}} \cos(Ft), \quad (36)$$

which is analogous to the solution of the damped harmonic motion in one dimension,

$$z(t) = Ge^{-\frac{\gamma t}{2}} \cos(\omega t + \phi), \quad (37)$$

where ω is the angular frequency and γ is the damping constant [8]. Even modifying the masses used in the first prototype, we still obtained a damped behavior. In other words, with the first prototype we were unable to verify the coupling of vertical oscillation with rotational oscillation, obtaining only a damped vertical mass-spring system. In fact, the procedure of finding a system where complete energy transfer occurs between the two types of harmonic motions, in which the oscillations are coupled, did not seem to be a trivial task.

As a preliminary result, we verified that the adjustment of the pendulum to occur the coupled oscillation depends on the moment of inertia of the support, the magnitude of the lateral masses, and the elastic constant of the spring, cf. discussed in Section 2.1.

We then analyze the second Wilberforce pendulum prototype, using the slinky spring with elastic constant of (0.53 ± 0.01) N/m (see Figure 2-B). The pendulum bob was made using a 30 cm acrylic ruler, and three markers as weights (Figure 2-B). Each pen has a width of (13.5 ± 0.05) cm, and a mass of (33.0 ± 0.5) g. As discussed in section 3.1, this total mass of (99.0 ± 0.5) g for the pendulum bob is out of linear regime of the Slinky spring. Using this prototype and the configuration of the experimental apparatus presented in Section 2.3, we obtained a result of the temporal evolution of the translation which is shown in Figure 6-B. This was the first result that suggested a coupled oscillation in z and in θ , being verified the gradual decrease in the amplitude of longitudinal motion up to the instant $t \approx 13$ s, with a subsequent increase in the amplitude.

Although the result obtained using the second prototype indicated the coupling of longitudinal and rotational motions, we could not verify with this prototype a reproducible result with well-described varying envelope, and we did not even obtain a periodic behavior with at least two nodes. This occurs mostly due to the use of masses above the linear spring regime, or a pendulum bob with an inadequate moment of inertia and the fact that the mass of the pendulum bob is out of the Slinky linear regime.

Finally, we set up the final prototype for the Wilberforce pendulum, which was used as the final apparatus for carrying out all the measurements and analyses presented below. The only difference between this prototype and the second one was the pendulum bob (see Figure 2-C).

Employing the final Wilberforce pendulum prototype, we obtained the translation and rotational motions that can be observed in Figures 7-A and 7-B, respectively.

For the translation motion, the curve fitting was achieved with an expression in the form

$$z(t) = A \cos(Bt) \cos(Ct), \quad (38)$$

with $A = (0.10 \pm 0.03)$ m, $B = (0.512 \pm 0.004)$ rad and $C = (4.802 \pm 0.004)$ rad/s. Eq. (38) is similar to Eq. (25), so that by comparison we have that $B = \omega_b/2$

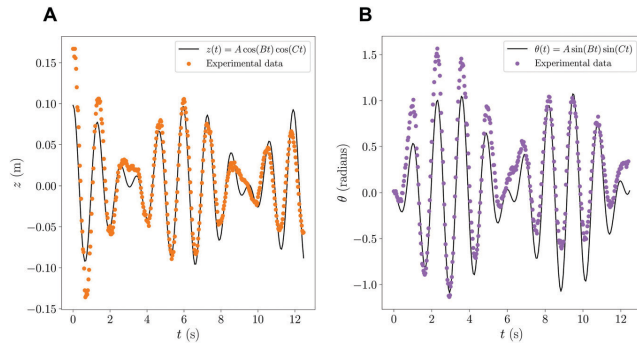


Figure 7: (A) Vertical z (in meters) and (B) angular θ (in radians) oscillation curves *versus* time (in seconds) obtained using the pendulum prototype shown in Fig. 2(C).

and $C = \omega$. Then we get

$$\omega_b = 1.024 \pm 0.008 \text{ rad/s}, \quad (39)$$

and

$$\omega = 4.802 \pm 0.004 \text{ rad/s}, \quad (40)$$

Regarding the result of the frequency ω_b in Eq. (24), we computed the value for the coupling constant

$$\epsilon = (11.06 \pm 0.09) \times 10^{-3} \text{ N}, \quad (41)$$

where the uncertainty was calculated from the error propagation, considering the uncertainties of the elastic constant and the moment of inertia. For comparison purposes, Berg and Marshall [3] obtained as a result $\epsilon = (9.27 \pm 0.30) \times 10^{-3} \text{ N}$, using a spring of steel, indicating that there is good agreement with our experimental results regarding the order of magnitude of the coupling constant.

Also using Eq. (24), we can evaluate the torsion constant of the spring, given by

$$\delta = \frac{\epsilon^2}{\omega_b^2 M}. \quad (42)$$

For this expression, we get the spring torsion constant for the slinky spring

$$\delta = (83 \pm 4) \times 10^{-4} \text{ N m}. \quad (43)$$

Considering now the results of ϵ and δ , we estimated the standard frequencies of oscillation using the definitions shown in Eqs. (11) and (12), which result in

$$\omega_z = 6.15 \pm 0.11 \text{ rad/s}, \quad (44)$$

$$\omega_\theta = 6.15 \pm 0.28 \text{ rad/s}. \quad (45)$$

As a result, the standard frequencies ω_z and ω_θ are in the same order of magnitude as ω (cf. Eq. (40)), with one difference on the order of 1.3 rad/s. Now analyzing the results for the rotational motion depicted in Figure 7-B,

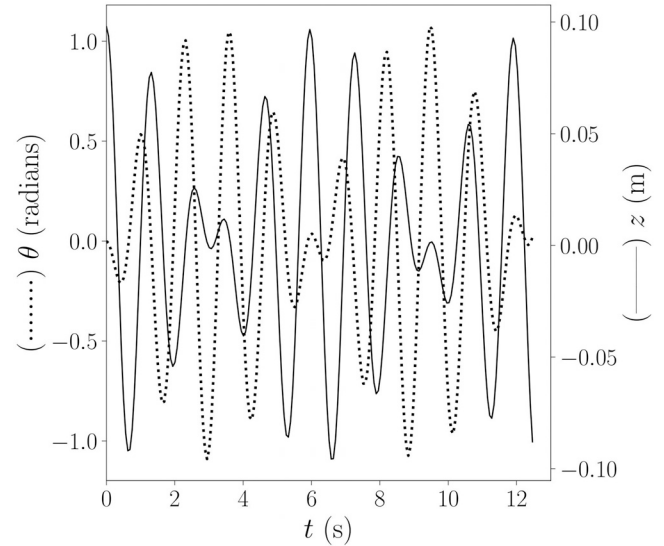


Figure 8: Curves of both vertical shift z (in meters, solid line) and angular displacement θ (in radians, dotted line) as a function of time (in seconds). The curves represent the fits obtained from the experimental data.

whose solution is described by Eq. (26)), we verified that the fit obtained by the curve fit function was of the

$$\theta(t) = A_2 \sin(Dt) \sin(Et), \quad (46)$$

where $D = B$, $E = C$. In fact, the result obtained by the adjustment was $D = (0.513 \pm 0.003) \text{ m}$ and $E = (4.802 \pm 0.004) \text{ rad/s}$, confirming the prediction of similarity between these parameters of the nonlinear fits. According to Eq. (22), we have that

$$A_2 = A \sqrt{\frac{M}{I}}, \quad (47)$$

from which we obtain an estimate for the amplitude of rotational motion

$$A_2 = (0.8 \pm 0.2) \text{ radians}, \quad (48)$$

with uncertainty calculated by error propagation. The result measured directly from the nonlinear fit was

$$A_2 = (1.09 \pm 0.03) \text{ radians}, \quad (49)$$

indicating that there is a good agreement between the predicted amplitude and that obtained from the experimental data. The implemented PYTHON notebook to fit the experimental curves of the coupled oscillations, as well as the "csv" files with the experimental data are available at [12]. A video showing the translation and rotational oscillation of the final setup of the Wilberforce pendulum can be watched at [13].

For the purpose of qualitative analysis, the adjustments of the longitudinal and rotational movements were superposed and the result is shown in Figure 8. Indeed, we can verify an energy transfer of longitudinal

elastic potential energy into the rotational elastic energy and vice versa. Moreover, we can note that the regions of maximum longitudinal amplitude coincide with the regions of minimum rotational amplitude, and that the longitudinal amplitude decreases as the rotational amplitude increases. Therefore, this result indicated that energy transfer was occurring and therefore the oscillations are coupled.

As a coarse estimation, we have computed the moment of inertia of the pendulum bob used in the second apparatus, and we got the value of $(3.51 \pm 0.05) \times 10^{-4}$ kg·m². Applying the Eq. (22), we estimate the A_2/A_1 ratio being equal to 16.8 ± 0.3 . For comparison purposes, this A_2/A_1 ratio for the final experimental setup (the third one) was estimated in 8.0 ± 0.8 . As a result, the A_2/A_1 ratio in the coupled oscillator was twice lower than the ratio for the uncoupled one. The M/I ratio is a relevant feature to predict the ratio of magnitudes of the coupled oscillations and verify if the experimental apparatus is suitable to address the coupling oscillation.

4. Conclusions

In summary, the Wilberforce pendulum has been implemented experimentally using a slinky plastic spring and a rod with weights at the ends. Although it appears to be a simple system to set up, there is an important experimental difficulty associated with the characteristics of the spring and the pendulum bob. Properties such as the elastic spring constant, as well as the mass and the moment of inertia of the pendulum bob were crucial to obtain resonant oscillators. Using an inclined plane mirror, and making the acquisition of images for both translation and rotational movements, we could get experimental data on the longitudinal (in z) and rotational (in θ) displacements. As a result, we obtained that the resonant frequency of the system was (4.802 ± 0.004) rad/s, showing a certain disparity with the estimated value which was in the order of 6.15 rad /s, although the results are in the same order of magnitude and we must disregard experimental inaccuracies. The amplitude of motion showed excellent agreement with the values measured from the adjustments by the non-linear least squares method, when compared to the predicted estimates. Thus, we see that the Wilberforce pendulum can be obtained using easily accessible materials, and the results can be used in quantitative studies of coupled oscillations.

Acknowledgments

The conceptualization of this work was proposed as part of the activities for the wave physics subject of the undergraduate physics course at UFABC. The authors gratefully thank professor Antônio Álvaro Ranha Neves for his critical comments and fruitful discussion. E.M.S.J.

acknowledges the financial support from the Brazilian agency FAPESP grant numbers 20/13172-8 and 2017/02317-2.

References

- [1] N.K. Bajaj, *The Physics of Waves and Oscillations* (Tata McGraw-Hill, New Delhi, 1988).
- [2] L.R. Wilberforce, *Philos. Mag.* **38**, 386 (1894).
- [3] R.E. Berg and T.S. Marshall, *Am. J. Phys.* **59**, 32 (1991).
- [4] P. Devaux, V. Piau, O. Vignaud, G. Grosse, R. Olarte and A. Nuttin, *Emerg. Sci.* **3**, 1 (2019).
- [5] M. Mewes, *Am. J. Phys.* **82**, 254 (2014).
- [6] T. Greczylo and E. Debowska, *Eur. J. Phys.* **23**, 441 (2002).
- [7] D.J. O'Brien, *Am. J. Phys.* **89**, 403 (2021).
- [8] H.M. Nussenzveig, *Curso de Física Básica: fluidos, oscilações e ondas, calor* (Edgard Blucher, São Paulo, 2018), v. 2.
- [9] D. Brown and A.J. Cox, *Phys. Teach.* **47**, 145 (2009).
- [10] Q. Wen and L. Yang, *Eur. J. Phys.* **42**, 064002 (2021).
- [11] N. Aranha, J.M.D. Oliveira Jr, L.O. Bellio and W. Bonventi Jr, *Rev. Bras. de Ensino de Fís.* **38**, e4305, 2016.
- [12] https://github.com/emarinhojr/wilberforce_pendulum_plots.
- [13] <https://www.youtube.com/watch?v=ImhrnjQ1OoM>.